Available online at www.sciencedirect.com

ScienceDirect

Energy Procedia 1 (2009) 479–486

Energy Procedia

www.elsevier.com/locate/procedia

GHGT-9

NiO particles with Ca and Mg based additives produced by spray-drying as oxygen carriers for chemical-looping combustion

Erik Jerndal[a,*], Tobias Mattisson[a], Ivo Thijs[b], Frans Snijkers[b], Anders Lyngfelt[a]

[a]*Chalmers University of Technology, S-412 96 Göteborg, Sweden*
[b]*VITO - Flemish Institute for Technological Research, B-2400 Mol, Belgium*

Abstract

Chemical-looping combustion is a two-step combustion process where CO_2 is obtained in a separate stream, ready for compression and sequestration. The technique involves two interconnected fluidized bed reactors, with a solid oxygen carrier circulating between them. Results of reactivity experiments with 24 different oxygen carriers, based on NiO with $NiAl_2O_4$ and/or $MgAl_2O_4$ and produced with spray-drying, are presented. The investigation revealed that oxygen carriers supported by $MgAl_2O_4$, or where a small amount of MgO was added, displayed an increased fuel conversion when compared to oxygen carriers of NiO supported by $NiAl_2O_4$.

Keywords: CO_2 capture; chemical-looping combustion; fluidized bed; oxygen carrier; spray-drying; NiO

1. Introduction

In chemical-looping combustion, CO_2 is separated from the rest of the flue gases without an energy consuming gas separation process. Hence, this technique has emerged as an attractive option to other CO_2 separation techniques, and as an alternative by which fossil fuels can be utilised without contributing to an increased atmospheric CO_2 concentration. The technique involves the use of metal oxide particles with the purpose of transferring oxygen from an air reactor to a fuel reactor. In the fuel reactor, the fuel in gaseous form reacts with the metal oxide according to reaction (1) and in the air reactor the reduced metal oxide is reoxidized according to reaction (2);

$$C_nH_{2m} + (2n+m)Me_xO_y \leftrightarrow nCO_2 + mH_2O + (2n+m)Me_xO_{y-1} \quad (1)$$

$$O_2 + 2Me_xO_{y-1} \leftrightarrow 2Me_xO_y \quad (2)$$

* Corresponding author. Tel.: +46-31-772 28 86
E-mail address: erik.jerndal@chalmers.se.

doi:10.1016/j.egypro.2009.01.064

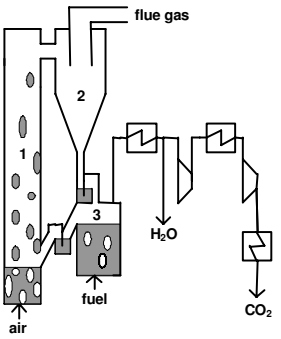

Figure 1. Schematic layout of the chemical-looping combustion process; 1) air reactor and riser, 2) cyclone and 3) fuel reactor.

The exit gas stream from the fuel reactor contains CO_2 and H_2O, which are separated in a condenser before CO_2 is compressed to a liquid, suitable for sequestration. The air reactor exhaust contains oxygen depleted air. The total amount of heat evolved from reaction (1) and (2) is the same as for traditional combustion, where the oxygen and fuel are in direct contact. A proposed design of the process is displayed in Figure 1 [1], where the air reactor is a riser with a gas velocity high enough to entrain the oxygen carrier particles. Oxidized particles are separated from the flue gases in a cyclone, and led to the fuel reactor where they are reduced by the gaseous fuel and transported back to the air reactor by gravitation. Particle locks prevent gas mixing between the two reactors. This design appears similar to a circulating fluidized bed boiler for solid fuels, thus using well proven technology and components [1].

The need to obtain suitable oxygen carrier materials has been identified as one of the key matters to further develop this technique [2]. Important criteria for the oxygen carriers are; high reactivity with fuel and oxygen as well as high fuel conversion, low fragmentation, attrition and agglomeration tendencies and low cost and environmental impact. Several transition state metals, primarily Ni, Cu, Mn and Fe can be used as oxygen carriers in chemical-looping combustion since they fulfil the above mentioned criteria to varying extents [3]. To increase the performance of these active materials, they should be supported by an inert material which provides a higher surface area for reaction and may act as a binder to increase their mechanical strength and hence their attrition resistance [3].

Ni generally has a high reaction rate with methane, the main component in natural gas and refinery gas, both during reduction and oxidation, and a high melting temperature which reduces the risk of agglomeration at high temperatures [4]. However, Ni is an expensive compound compared to other proposed oxygen carrier materials. Also, the need of preparing oxygen carriers from commercially available Ni sources and with low cost production methods is obvious. Other factors needed to consider when using Ni are; the comparatively higher toxicity and the lower methane conversion, which is limited to 99% at 950ºC.

Oxygen carriers for chemical-looping combustion based on NiO supported by $NiAl_2O_4$ were first proposed by Jin et al. [5] in 1999 and are among the most frequently studied oxygen carriers. This material combination has sustained continuous operation for 100 h in a 10 kW circulating prototype unit with excellent results [6], without displaying any significant difference in chemical composition, structure or reactivity [7]. The reduction and oxidation reactions of these oxygen carriers have been studied in detail by Mattisson et al. [8] and the range of suitable operating conditions in a chemical-looping combustion process with respect to solids inventories have been investigated by Abad et al. [4]. An overview of the publications on experimental oxygen carrier data is given by Johansson et al. [9].

In earlier studies it has been concluded that high performance oxygen carriers of NiO, supported by $NiAl_2O_4$, can be prepared from commercially available raw materials by the small-scale method freeze-granulation [10] and that similar particles can be prepared by spray-drying [11], which is a method well suited for large-scale production. The aim of the present investigation is to study if the performance of spray-dried oxygen carriers can be further increased, with respect to their fuel conversion, by using a magnesium-containing support material. Such improvements have earlier been shown for freeze-granulated particles [10, 12]. Some of the particles were also prepared with a small addition of $Ca(OH)_2$ since an earlier study showed that this increases the physical strength of the oxygen carriers [10].

2. Preparation of oxygen carriers

Spherical oxygen carrier particles were prepared by the industrial spray-drying method, using commercial raw or semi-finished materials, as presented in Table 1. All materials were prepared to give an active NiO content of 40%, based on weight. For the materials where α-Al_2O_3 was included in the preparation phase the alumina reacted

completely to $NiAl_2O_4$ during heat treatment and hence excess NiO was added to obtain free NiO in the sample. The additions of MgO and $Ca(OH)_2$ presented in Table 1 are mass fractions based on the total raw material and it is believed that these additions result in formation of the inert spinels $MgAl_2O_4$ and $CaAl_2O_4$ respectively.

Table 1. Raw materials used in oxygen carrier production.

Oxygen Carrier	NiO	Support 1	Support 2	Support 3
S1	Novamet Refractory grade	α-Al_2O_3, CTC3000sg	5% MgO, Magchem30	
S2	OMG Standard grade	α-Al_2O_3, CTC3000sg	5% MgO, Magchem30	1% $Ca(OH)_2$, Nordkalk
S3	Novamet Refractory grade	$MgAl_2O_4$, CTC55		
S4	OMG Standard grade	$MgAl_2O_4$, CTC55		
S5	Novamet Refractory grade	α-Al_2O_3, CTC3000sg	1% MgO, Magchem30	
S6	Novamet Refractory grade	$MgAl_2O_4$, E-SY2000		
S7	Novamet Refractory grade	$MgAl_2O_4$, AR78		
S8	Novamet Refractory grade	α-Al_2O_3, CTC3000sg	10% MgO, Magchem30	
S9	OMG Standard grade	α-Al_2O_3, CTC3000sg	1% $Ca(OH)_2$, Nordkalk	
NOV1sd	Novamet Refractory grade	α-Al_2O_3, CTC3000sg		

The particle preparation was performed in the following manner; a powder mixture of NiO and varying support materials were dispersed in deionized water containing polyethyleneoxide and/or polyvinylalcohol and/or polyethyleneglycol as organic binders and Darvan C or Dolapix as dispersant. The suspension was homogenized by milling and the water-based suspension was continuously stirred with a propeller blade mixer while being pumped to the 2-fluid spray-dry nozzle. Sintering of the oxygen carriers was performed in air at top temperatures in the range of 1300°C to 1600°C, for 4 hours. This sintering temperature is displayed in an abbreviation for each oxygen carrier in Table 2. Totally, 24 oxygen carrier materials were produced in this manner and are displayed along with NOV1sd which was prepared without additives in an earlier study and is included here for comparison [11].

Table 2. Physical properties of particles produced.

Oxygen Carrier	Crushing Strength [N]	Apparent Density [kg/m^3]	Oxygen Carrier	Crushing Strength [N]	Apparent Density [kg/m^3]
S1T1400	2.0	2850	S7T1400	2.1	2920
S1T1450	3.4	3360	S7T1450	3.1	3060
S2T1400	0.5	2040	S7T1500	3.5	3230
S2T1500	1.6	3360	S8T1400	2.5	2910
S2T1600	2.8	3950	S8T1450	3.9	3480
S3T1400	1.3	2850	S8T1500	5.0	3740
S4T1400	-	2070	S9T1300	-	1800
S4T1500	0.1	2220	S9T1400	0.2	2070
S4T1600	0.3	2530	S9T1500	1.1	3180
S5T1400	1.6	2970	NOV1T1400sd	1.6	2900
S5T1500	2.7	3290	NOV1T1425sd	1.8	2990
S5T1600	3.6	3660	NOV1T1450sd	1.8	3190
S6T1400	1.6	2990	NOV1T1475sd	2.7	3470
S6T1450	2.5	3200	NOV1T1500sd	3.0	3550
S6T1500	3.5	3470			

3. Experimental

To avoid major fragmentation and attrition in a real chemical-looping system, it is likely that oxygen carriers need to possess certain strength. Thus, the crushing strength, or the force needed to fracture the particles, was measured as an average of 30 fractured particles sized 180-212 µm, using a Shimpo FGN-5 device. Also, the apparent density of all the fresh particles, sized 125-180 µm, was measured. Here, a void factor of 0.37 was assumed, since this is the theoretic voidage of a normally packed bed with uniformly sized spherical particles.

The reactivity investigations were conducted in a fluidized bed reactor of quartz, with a length of 870 mm and an inner diameter of 22 mm. The reactor had a porous quartz plate placed 370 mm from the bottom, and the temperature was measured 5 mm under and 25 mm above this plate. The bed material, sized 125-180 µm, was placed on the porous plate and heated in an electric oven while being exposed to an inert atmosphere of N_2, until reaching a desired reaction temperature of 950ºC. After heat-up, the particles were exposed alternately to 5% O_2 in N_2 and 100% CH_4, thus simulating the cyclic conditions of a chemical-looping combustion system. To avoid mixing of O_2 and CH_4 during transition between oxidation and reduction, N_2 was introduced for 180 s after each period. The inlet gas flow was 450 mL_N/min during reduction and inert periods and 1000 mL_N/min during oxidation where the flows are normalized to 1 bar and 0ºC. These flows correspond to a u/u_{mf} of 3.4-3.9 during reduction and 10.8-12.7 during oxidation, where u is the incoming gas velocity and u_{mf} is the theoretic minimum fluidization velocity [13].

The gas from the reactor was led to an electric cooler, where the water produced in the reduction was condensed and removed, and then on to a Rosemount NGA-2000 gas analyzer, where the concentrations of CO_2, CO, CH_4 and O_2 as well as the flow were measured.

The degree of oxidation of the oxygen carriers, or the conversion, is defined in equation (3), where m is the actual mass of the sample, m_{ox} is the mass of the sample when fully oxidized, and m_{red} the mass of the sample in the fully reduced form. To quantify the amount of unreacted methane leaving the reactor, a ratio of methane fraction in the outlet gas stream was defined according to equation (4) and a gas yield for the reduction period was defined as the degree of incoming methane that had been completely converted to CO_2, as defined in equation (5). In these equations, p_i denotes the partial pressure of component i in the outlet gas stream.

$$X = \frac{m - m_{red}}{m_{ox} - m_{red}} \quad (3) \qquad fr_{CH_4} = \frac{p_{CH_4}}{p_{CH_4} + p_{CO_2} + p_{CO}} \quad (4) \qquad \gamma_{red} = \frac{p_{CO_2}}{p_{CH_4} + p_{CO_2} + p_{CO}} \quad (5)$$

In order to facilitate comparison between different oxygen carriers, a methane index was introduced, defined as the fraction of methane leaving the reactor when X was between 0.95 and 0.99. These values of conversion, X, were chosen since an initial methane peak appeared somewhere in this interval for all oxygen carriers studied. The methane index was calculated as;

$$CH_4, index = \frac{\int_{X=0.95}^{X=0.99} (p_{CH_4}) dX}{\int_{X=0.95}^{X=0.99} (p_{CH_4} + p_{CO_2} + p_{CO}) dX} \quad (6)$$

4. Results and discussion

Of the 24 oxygen carriers prepared, 15 were based on Novamet Refractory grade and 9 were based on OMG Standard grade as active NiO. The apparent density and crushing strength as a function of sintering temperature for the materials based on Novamet Refractory grade NiO are displayed in Figure 2. Also included is NOV1sd which was prepared without additives in an earlier study [11], and is included here for comparison reasons. As seen, both the density and the crushing strength increases with an increased sintering temperature and the density is not drastically altered when additives are included or when $MgAl_2O_4$ is used as supporting agent while the crushing strength is generally somewhat higher.

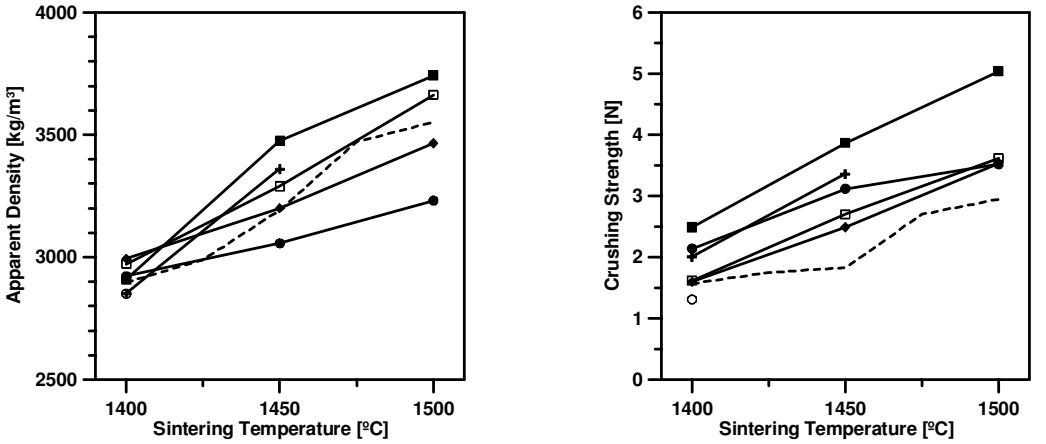

Figure 2. Apparent density and crushing strength as a function of sintering temperature for S1(+), S3(○), S5(□), S6(◆), S7(●), S8(■) and NOV1sd(---).

Apparent density and crushing strength for the oxygen carriers based on OMG Standard grade are displayed in Figure 3. Two of the materials, S4T1400 and S9T1300 were too soft to give distinct values during crushing strength measurements and such values are therefore not displayed for these. Interestingly, all materials based on OMG Standard grade have similar density when sintered at 1400ºC while for materials sintered at higher temperatures, particles where $Ca(OH)_2$ was added displays a higher apparent density. Moreover, the crushing strength is highest for the materials prepared with a combination of $Ca(OH)_2$ and MgO addition. The material prepared with commercial $MgAl_2O_4$, i.e. S4, had a very low crushing strength, even when sintered at 1600ºC.

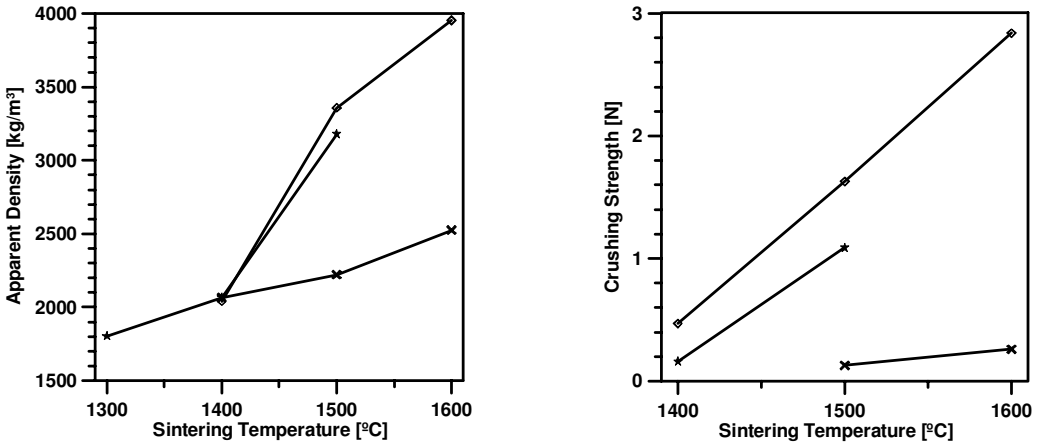

Figure 3. Apparent density and crushing strength as a function of sintering temperature for S2(◇), S4(✕) and S9(★).

The main reason for preparing oxygen carriers based on NiO with magnesium-containing support materials was to increase the fuel conversion early in reduction, which is limited for NiO oxygen carriers supported by $NiAl_2O_4$ [12, 14]. The fact that unconverted methane appears when the oxygen carriers are highly oxidized, but disappears as the conversion of the particles decreases, suggests that its presence is caused by the limited number of metallic Ni sites, which acts as catalyst for converting methane. The fraction of unreacted methane detected in the outlet of the reactor for seven of the oxygen carriers is displayed in Figure 4. Also included for comparison is NOV1T1450sd. S4

and S9 are not included in the figure since their crushing strength was believed to be too low to withstand fragmentation and attrition in a large-scale application. As is evident, all materials studied displayed a significant improvement in methane conversion when compared to NOV1T1450sd. A quantification of this improvement is displayed as a methane index for each oxygen carrier.

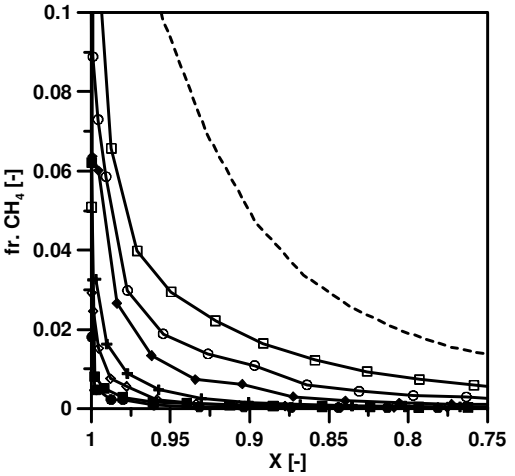

Oxygen Carrier	CH_4, index [%]
NOV1T1450sd	10
S5T1400	3.9
S3T1400	2.5
S6T1400	1.6
S1T1400	0.69
S2T1500	0.36
S8T1400	0.21
S7T1400	0.13

Figure 4. Fraction of unreacted CH_4 as a function of oxygen carrier conversion, X, and $CH_{4,index}$ for NOV1T1450sd(---), S5T1400(□), S3T1400(○), S6T1400(◆), S1T1400(+), S2T1500(◇), S8T1400(■) and S7T1400(●).

Each of these oxygen carriers have been tested for 11 to 13 consecutive reduction and oxidation cycles, where the time in reduction was gradually increased until full oxygen carrier conversion was reached. The time in oxidation was always long enough to give fully oxidized particles. During these tests, no defluidization tendencies occurred for any of the oxygen carriers, which was the case for NOV1T1450sd when tested at the same conditions [11]. This suggests that; besides increasing the CH_4 conversion, an addition of MgO also seem to improve the fluidization behaviour. The fraction of unreacted CH_4 was fairly unchanged as a function of reduction cycle for all these materials although the conversion to CO_2 was not, as displayed in Figures 5 and 6. These figures show the gas yield as a function of oxygen carrier conversion for all reduction cycles that were long enough to be terminated at low gas yields. All materials displayed the same trend of increasing their oxygen carrier conversion span where the gas yield was high as a function of reduction number, i.e. the number of reduction increases to the right in all figures.

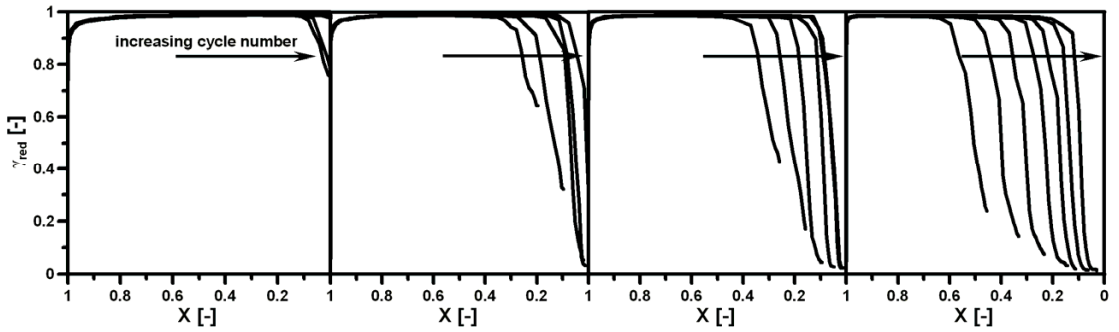

Figure 5. Gas yield, $\gamma_{red,}$ as a function of oxygen carrier conversion, X, for S5T1400, S3T1400, S6T1400 and S1T1400.

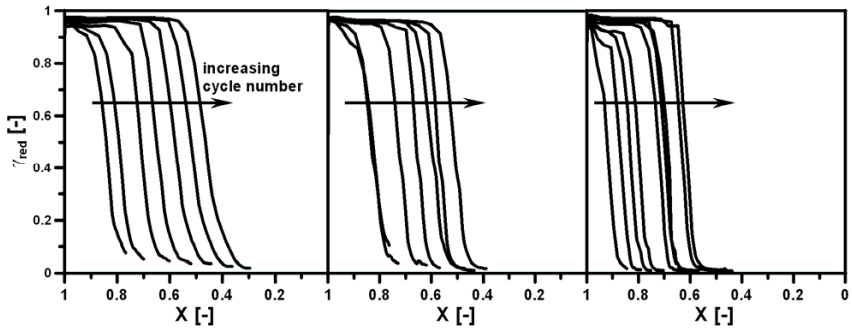

Figure 6. Gas yield, γ_{red}, as a function of oxygen carrier conversion for S2T1500, S8T1400 and S7T1400.

As seen in Figures 5 and 6, the gas yield does not reach 100% for any of these oxygen carriers. The reason for this is the thermodynamic fuel conversion restraint when NiO is used as the active material in the oxygen carriers. Interestingly, oxygen carriers with a high methane index also have a high gas yield for a large oxygen carrier conversion span. This statement also applies the other way around; oxygen carriers with low methane index also have a low conversion span, where the gas yield is high. In fact, a rank of the oxygen carrier's methane index and conversion span with high gas yield follows exactly the same order. The reason for this is not well known but is believed to be caused by a decreased internal transport in the oxygen carriers with low methane index. A decreased internal transport is believed to give a higher ratio of nickel on the surface of the oxygen carrier and hence an increased catalytic effect in converting CH_4. However, the decreased internal transport seems to limit the conversion to CO_2, which results in major CO formation for these oxygen carriers at low degrees of oxidation. The implication of this in a real application is that a high circulation rate is necessary to maintain a high fuel conversion. However, it should be pointed out that the improved gas yield as a function of cycle number showed no tendencies of slowing down and therefore even the oxygen carriers with a low methane index might give high gas yields at low degrees of oxygen carrier oxidation eventually.

One of these materials, S1T1400, has been investigated by Linderholm et al. in continuous operation in a 10 kW unit using natural gas [15]. Here, it was referred to as N-VITOMg and combined with NOV1T1450, referred to as N-VITO. The increased fuel conversion when adding a magnesium-containing oxygen carrier was clearly confirmed.

As determined from analysis using a FEI, Quanta 200 Environmental Scanning Electron Microscope FEG, all materials maintained their spherical shape during reactivity testing although their surface structure changed at varying degree. Figure 7 displays SEM-images of the surface structure of two of the materials, S1 and S7, prior to and after reactivity testing. The most obvious change is seen for S7 which might explain the major improvement in gas conversion for this oxygen carrier.

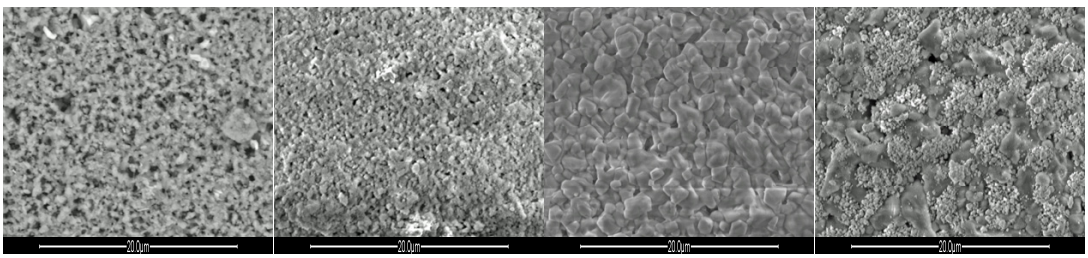

Figure 7. SEM-images of S1 prior to- and after reactivity testing and S7 prior to- and after reactivity testing. The bottom bar is 20 µm.

5. Conclusions

Physical properties and fuel conversion of totally 24 oxygen carriers produced by spray-drying with NiO as active material have been investigated. These materials were prepared with different amounts of additives or support materials with high content of Mg or Ca and compared to materials without additives composed of NiO supported by $NiAl_2O_4$. Materials with MgO added in the particle preparation or with high Mg content in the support material gave a considerably increased fuel conversion when the oxygen carrier was highly oxidized. Oxygen carriers with a high methane conversion generally had low conversion to CO_2 at low degrees of oxygen carrier oxidation. However, the conversion to CO_2 increased as a function of cycle for all oxygen carriers investigated while the fraction of unreacted CH_4 was fairly unchanged.

Acknowledgements

This work was part of the EU financed project Chemical Looping Combustion CO_2-Ready Gas Power (CLC Gas Power, EU contract: 019800) led by Chalmers University of Technology. The project is also part of phase II of CCP (CO_2 Capture Project) via Shell.

References

1 Lyngfelt, A., Leckner, B., Mattisson, T. A Fluidized-Bed Combustion Process with Inherent CO_2 Separation; Application of Chemical-Looping Combustion. *Chemical Engineering Science*, 2001, **56**(10), 3101-3113.

2 Lyngfelt, A., Johansson, M., Mattisson, T. Chemical-Looping Combustion - Status of Development. *9th International Conference on Circulating Fluidized Beds May 13 -16, Hamburg*, 2008.

3 Adanez, J., de Diego, L. F., Garcia-Labiano, F., Gayan, P., Abad, A., Palacios, J. M. Selection of Oxygen Carriers for Chemical-Looping Combustion. *Energy & Fuels*, 2004, **18**(2), 371-377.

4 Abad, A., Adanez, J., Garcia-Labiano, F., de Diego, L. F., Gayan, P., Celaya, J. Mapping of the Range of Operational Conditions for Cu-, Fe-, and Ni-Based Oxygen Carriers in Chemical-Looping Combustion. *Chemical Engineering Science*, 2007, **62**(1-2), 533-549.

5 Jin, H., Okamoto, T., Ishida, M. Development of a Novel Chemical-Looping Combustion: Synthesis of a Solid Looping Material of $NiO/NiAl_2O_4$. *Industrial & Engineering Chemistry Research*, 1999, **38**(1), 126-132.

6 Lyngfelt, A., Thunman, H. Construction and 100 h of Operational Experience of a 10-kW Chemical-Looping Combustor. *Carbon Dioxide Capture for Storage in Deep Geologic Formations-Results from the CO_2 Capture Project*, 2005, **1**, 625-645.

7 Johansson, M., Mattisson, T., Lyngfelt, A. Use of $NiO/NiAl_2O_4$ Particles in a 10 kW Chemical-Looping Combustor. *Industrial & Engineering Chemistry Research*, 2006, **45**(17), 5911-5919.

8 Mattisson, T., Johansson, M., Jerndal, E., Lyngfelt, A. The Reaction of NiO/Al_2O_3 Particles with Alternating Methane and Oxygen. *Accepted for Publication in Canadian Journal of Chemical Engineering*, 2007.

9 Johansson, M. Screening of oxygen-carrier particles based on iron-, manganese-, copper- and nickel oxides for use in chemical-looping technologies. *Dept. of Chemical and Biological Engineering, Environmental Inorganic Chemistry, Chalmers University of Technology, Göteborg, Sweden, PhD Thesis*, 2007.

10 Jerndal, E., Mattisson, T., Lyngfelt, A. Investigation of Different $NiO/NiAl_2O_4$ Particles as Oxygen Carriers for Chemical-Looping Combustion. *submitted for publication*, 2008.

11 Jerndal, E., Mattisson, T., Thijs, I., Snijkers, F., Lyngfelt, A. Investigation of $NiO/NiAl_2O_4$ Oxygen Carriers for Chemical-Looping Combustion Produced by Spray-Drying. *submitted for publication*, 2008.

12 Johansson, M., Mattisson, T., Lyngfelt, A., Abad, A. Using Continuous and Pulse Experiments to Compare two Promising Nickel-Based Oxygen Carriers for use in Chemical-Looping Technologies. *Fuel Processing Technology*, 2008, **87**(6), 988-1001.

13 Kunii, D., Levenspiel, O. Fluidization Engineering. *Butterworth-Heinman*, 1991.

14 Mattisson, T., Johansson, M., Lyngfelt, A. The Use of NiO as an Oxygen Carrier in Chemical-Looping Combustion. *Fuel*, 2006, **85**(5-6), 736-747.

15 Linderholm, C., Mattisson, T., Lyngfelt, A. Long-Term Integrity Testing of Spray-Dried Particles in a 10 kW Chemical-Looping Combustor using Natural Gas as Fuel. *submitted for publication*, 2008.